The NuRD chromatin–remodeling complex regulates signaling and repair of DNA damage

Godelieve Smeenk,[1] Wouter W. Wiegant,[1] Hans Vrolijk,[2] Aldo P. Solari,[3] Albert Pastink,[1] and Haico van Attikum[1]

[1]Department of Toxicogenetics, [2]Department of Molecular Cell Biology, and [3]Department of Medical Statistics, Leiden University Medical Center, Leiden 2300RC, Netherlands

Cells respond to ionizing radiation (IR)–induced DNA double-strand breaks (DSBs) by orchestrating events that coordinate cell cycle progression and DNA repair. How cells signal and repair DSBs is not yet fully understood. A genome-wide RNA interference screen in *Caenorhabditis elegans* identified *egr-1* as a factor that protects worm cells against IR. The human homologue of *egr-1*, MTA2 (metastasis-associated protein 2), is a subunit of the nucleosome-remodeling and histone deacetylation (NuRD) chromatin-remodeling complex. We show that knockdown of MTA2 and CHD4 (chromodomain helicase DNA-binding protein 4), the catalytic subunit (adenosine triphosphatase [ATPase]) of NuRD, leads to accumulation of spontaneous DNA damage and increased IR sensitivity. MTA2 and CHD4 accumulate in DSB-containing chromatin tracks generated by laser microirradiation. Directly at DSBs, CHD4 stimulates RNF8/RNF168-dependent formation of ubiquitin conjugates to facilitate the accrual of RNF168 and BRCA1. Finally, we show that CHD4 promotes DSB repair and checkpoint activation in response to IR. Thus, the NuRD chromatin–remodeling complex is a novel regulator of DNA damage responses that orchestrates proper signaling and repair of DSBs.

Introduction

The efficient and accurate repair of chromosomal double-strand breaks (DSBs), which may arise from exposure to agents such as ionizing radiation (IR), is critical in maintaining genome stability and preventing cell death and carcinogenesis. To avoid deleterious effects of DSBs, eukaryotic cells activate signaling cascades, called checkpoints, which coordinate rapid detection of DNA breaks with a temporal arrest in cell cycle progression and activation of DNA repair mechanisms (Hoeijmakers, 2001; Khanna and Jackson, 2001).

The cellular response to DSBs is predominantly coordinated by the phosphatidylinositol 3-kinase–like kinases ataxia telangiectasia mutated (ATM) and ataxia telangiectasia and Rad3 related (ATR). ATM phosphorylates histone H2AX (γH2AX) in DSB-flanking chromatin to create an environment that allows for the spatiotemporal redistribution and accumulation of checkpoint and DNA repair factors at DNA breaks (van Attikum and Gasser, 2009). Among the first proteins to arrive at DSBs is MDC1, which directly binds to γH2AX (Stucki et al., 2005). This allows for the recruitment of the E2 ubiquitin conjugase UBC13 and the E3 ubiquitin ligase RNF8, the latter of which binds to MDC1 (Huen et al., 2007; Kolas et al., 2007; Mailand et al., 2007). RNF8/UBC13 promote the ubiquitylation of histones H2A/H2AX, leading to the recruitment of another E3 ubiquitin ligase, RNF168, which associates with RNF8-ubiquitylated histones via its ubiquitin-interacting motifs (Huen et al., 2007; Kolas et al., 2007; Mailand et al., 2007; Doil et al., 2009; Stewart et al., 2009). RNF168 cooperates with UBC13 to amplify RNF8-mediated histone ubiquitylation to a threshold required for the accumulation of checkpoint and repair proteins, including BRCA1, 53BP1, RAD18, and PTIP, in the DSB-flanking chromatin compartment (Wang and Elledge, 2007; Doil et al., 2009; Gong et al., 2009; Huang et al., 2009; Stewart et al., 2009). In addition to these ATM-driven events, DSB ends undergo extensive resection, leading to the formation of replication protein A–coated single-stranded DNA and subsequent assembly and activation

Correspondence to Haico van Attikum: h.van.attikum@lumc.nl

Abbreviations used in this paper: ATM, ataxia telangiectasia mutated; ATR, ataxia telangiectasia and Rad3 related; DDR, DNA damage response; DSB, double-strand break; IR, ionizing radiation; IRIF, IR-induced foci; NuRD, nucleosome remodeling and histone deacetylation; TERT, telomerase reverse transcriptase; WCE, whole cell extract.

The Rockefeller University Press $30.00
J. Cell Biol. Vol. 190 No. 5 741–749
www.jcb.org/cgi/doi/10.1083/jcb.201001048

of ATR (Zou and Elledge, 2003; Jazayeri et al., 2006; Dubrana et al., 2007). Finally, ATM and ATR amplify the signals generated at DSBs by phosphorylating several regulatory proteins, including SMC1, CHK1, CHK2, p53, and p21, that coordinate cell cycle progression or induce apoptosis (Khanna and Jackson, 2001; Shiloh, 2003).

The cross talk between histone modifications (e.g., phosphorylation and ubiquitylation) in DSB-flanking chromatin controls ATM/ATR-dependent signaling and repair of DSBs, yet it is unclear how this is achieved (van Attikum and Gasser, 2009). One possible mechanism may be ATP-dependent chromatin remodeling performed by ATPases of the SNF2 superfamily (Clapier and Cairns, 2009). We and others have previously demonstrated in budding yeast that several chromatin-remodeling complexes (INO80, SWR1, SWI/SNF, and RSC) are recruited to DSBs, where they change chromatin structure in distinct ways to regulate cell cycle progression and/or DSB repair (Morrison et al., 2004; van Attikum et al., 2004, 2007; Chai et al., 2005; Shim et al., 2005, 2007; Tsukuda et al., 2005; Papamichos-Chronakis et al., 2006; Liang et al., 2007). In contrast to budding yeast, in human cells, the role of chromatin remodeling during the cellular response to DSBs is just beginning to emerge. The TIP60 and SWI/SNF chromatin-remodeling complexes, for example, have been implicated in DNA repair by promoting histone acetylation and H2AX phosphorylation at DSBs, respectively (Murr et al., 2006; Park et al., 2006; Ikura et al., 2007), whereas ALC1 has recently been shown to assist in poly(ADP-ribose) polymerase–dependent chromatin remodeling at sites of DNA damage (Ahel et al., 2009; Gottschalk et al., 2009). However, it is unclear how the interplay between chromatin remodeling and histone modifications at DSBs coordinates cell cycle progression and DNA repair.

In this study, we identify the nucleosome-remodeling and histone deacetylation (NuRD) complex as a novel regulator of the DSB response in human cells. NuRD prevents the accumulation of spontaneous DNA damage and regulates apoptotic responses through p53 and p21. Moreover, NuRD is rapidly recruited to DSBs, where it promotes RNF8/RNF168-mediated histone ubiquitylation and the ubiquitin-dependent accumulation of RNF168 and BRCA1. Consequently, loss of NuRD components causes defects in DNA repair and checkpoint activation, rendering cells hypersensitive to IR. Thus, the NuRD chromatin–remodeling complex is a novel DNA damage response (DDR) factor that helps to preserve genome stability by regulating signaling and repair of DNA damage.

Results and discussion

CHD4 preserves genome stability and prevents apoptosis

We previously performed a genome-wide RNAi screen in the nematode *Caenorhabditis elegans* and identified 45 genes that protect worms against IR (van Haaften et al., 2006). Among these genes were well-known DDR factors and several novel genes, including *egr-1/lin-40*. *egr-1* encodes for a protein that is homologous to MTA2 (metastasis-associated protein 2), which is a component of the human NuRD complex (Xue et al., 1998; Zhang et al., 1999). A biochemical study indicated that MTA2 modulates the histone deacetylation activity of NuRD (Zhang et al., 1999). The chromatin-remodeling activity of this complex resides within another subunit, CHD4 (chromodomain helicase DNA-binding protein 4), which was first identified as a dermatomyositis-specific autoantigen (Seelig et al., 1995). CHD4 is a member of the SNF2 family of ATPases and possesses intrinsic ATP-dependent nucleosome-remodeling activity (Wang and Zhang, 2001). It is thought that NuRD represses transcription by regulating chromatin structure (Denslow and Wade, 2007). Moreover, a recent study showed that loss of several NuRD components results in chromatin defects that are associated with DNA damage accumulation and aging (Pegoraro et al., 2009). However, whether NuRD preserves genome stability and regulates the DDR remained unclear.

To investigate this, we transfected U2OS cells with siRNAs against luciferase or CHD4 and counted cells 2, 3, and 4 d after siRNA treatment. CHD4 knockdown cells proliferated much slower than control cells (Fig. 1, A and B). Flow cytometric analysis of these cells did not show any significant changes in cell cycle distribution. However, morphological changes and marked sub-G1 peaks, indicative of apoptosis, were observed 2–4 d after siRNA transfection (Fig. 1, B and C). Consistently, the levels of p53, phosphorylated p53 (S15p), and the p53 effector p21, which coordinate cell cycle progression and apoptosis, were significantly increased in the absence of CHD4 (Fig. 1 D), which is in agreement with an earlier study implicating a role for NuRD in apoptosis and p53/p21 regulation (Luo et al., 2000). We investigated whether apoptosis induced by loss of CHD4 might be related to the spontaneous occurrence of DNA lesions. Indeed, CHD4 knockdown cells showed increased levels of γH2AX as early as 2 d after siRNA transfection (Fig. 1 D), corroborating findings from a recent study (Pegoraro et al., 2009). Thus, CHD4 depletion leads to the accumulation of spontaneous DNA damage and activation of the apoptotic p53/p21 program. We infer that NuRD prevents genome instability and apoptosis.

CHD4 and MTA2 protect cells against the clastogenic effects of IR

EGR-1 (MTA2) protects worm cells against IR (van Haaften et al., 2006). To examine whether MTA2 also protects human cells against IR, we tested whether its depletion affects clonogenic survival of VH10-SV40 cells. Loss of MTA2 led to an increase in IR sensitivity that was comparable with that observed in XRCC4 knockdown cells, which are impaired in DSB repair by nonhomologous end joining (Fig. 1, E and F; Grawunder et al., 1998). In addition, we found that CHD4-depleted cells show increased IR sensitivity (Fig. 1, E and G). Thus, both MTA2 and CHD4 protect cells against the effects of IR, implicating a role for NuRD in the cellular response to DSBs. Furthermore, MTA2 protects both worm and human cells against IR, which may suggest that its putative role in the DDR is conserved.

CHD4 controls the p53/p21 axis of the IR-induced DDR

To investigate the role of NuRD in the DDR, we examined whether CHD4 depletion affects ATM/ATR-dependent phosphorylation

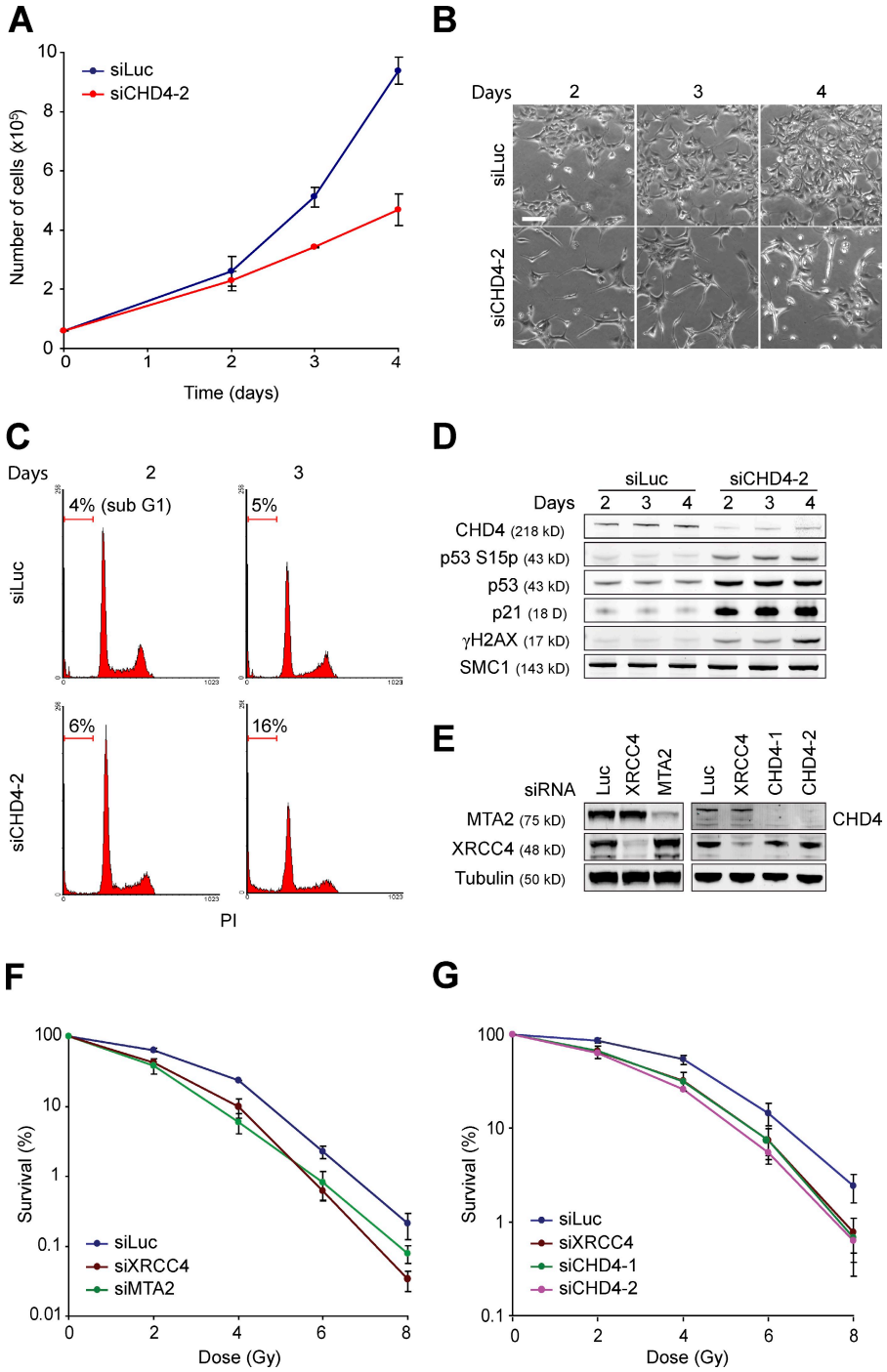

Figure 1. **MTA2 or CHD4 depletion renders cells sensitive to IR.** (A) Depletion of CHD4 reduces cell proliferation. U2OS cells were transfected with the indicated siRNAs. Cells were counted 0, 2, 3, and 4 d after siRNA transfection. (B) Pictures from representative areas of the cell dishes from A are shown. Bar, 200 µm. (C) FACS analysis of cells from A. PI, propidium iodide. (D) CHD4 depletion leads to enhanced levels of phosphorylated p53 (S15p), p53, p21, and γH2AX. Protein levels were monitored by Western blot analysis using WCEs from cells in A. SMC1 is a loading control. (E) CHD4, MTA2, and XRCC4 levels were monitored by Western blot analysis using WCEs of cells in F and G. Tubulin is a loading control. (F) MTA2 depletion renders cells hypersensitive to IR. VH10-SV40 cells were transfected with the indicated siRNAs. (G) CHD4 depletion renders cells hypersensitive to IR. As in F, except that siRNAs against CHD4 were used. Graphs represent the mean ± SEM of three independent experiments.

of DDR components in response to IR. Knockdown of CHD4 did not impair IR-induced ATM activation or γH2AX formation, but led to increased levels of γH2AX in unirradiated cells, corroborating our previous result (Fig. 1 D, Fig. 2 A, and Fig. S1). We then investigated whether CHD4 mediates ATM/ATR-dependent activation of downstream effectors SMC1 (S966p), CHK1 (S317p), CHK2 (S19p), p53 (S15p), and p21 of the DDR. We repeatedly observed a small increase in the phosphorylation of SMC1 and CHK1, but not of CHK2 within the first 30 min after IR exposure (unpublished data). In addition, we observed a small accumulation of CHD4-depleted cells in mid–S phase, suggesting that this aberration in the phosphorylation status of SMC1 and CHK1, which are regulators of IR-induced intra–S phase checkpoints, has a weak effect on cell cycle progression (Fig. 2, B and C). However, loss of CHD4 enhanced the levels of total p53 and phosphorylated p53 after exposure to IR. This was accompanied by an increase in p21 levels 24 h after IR treatment (Fig. 2 A). p53 and p21 play a prominent role in the G1 checkpoint response (Khanna and Jackson, 2001; Shiloh, 2003). Accordingly, we detected an arrest of CHD4-depleted cells in G1 phase that was maintained after IR exposure (Fig. 2, B and C). This suggests that CHD4 controls p53/p21-dependent G1 checkpoint responses induced by IR.

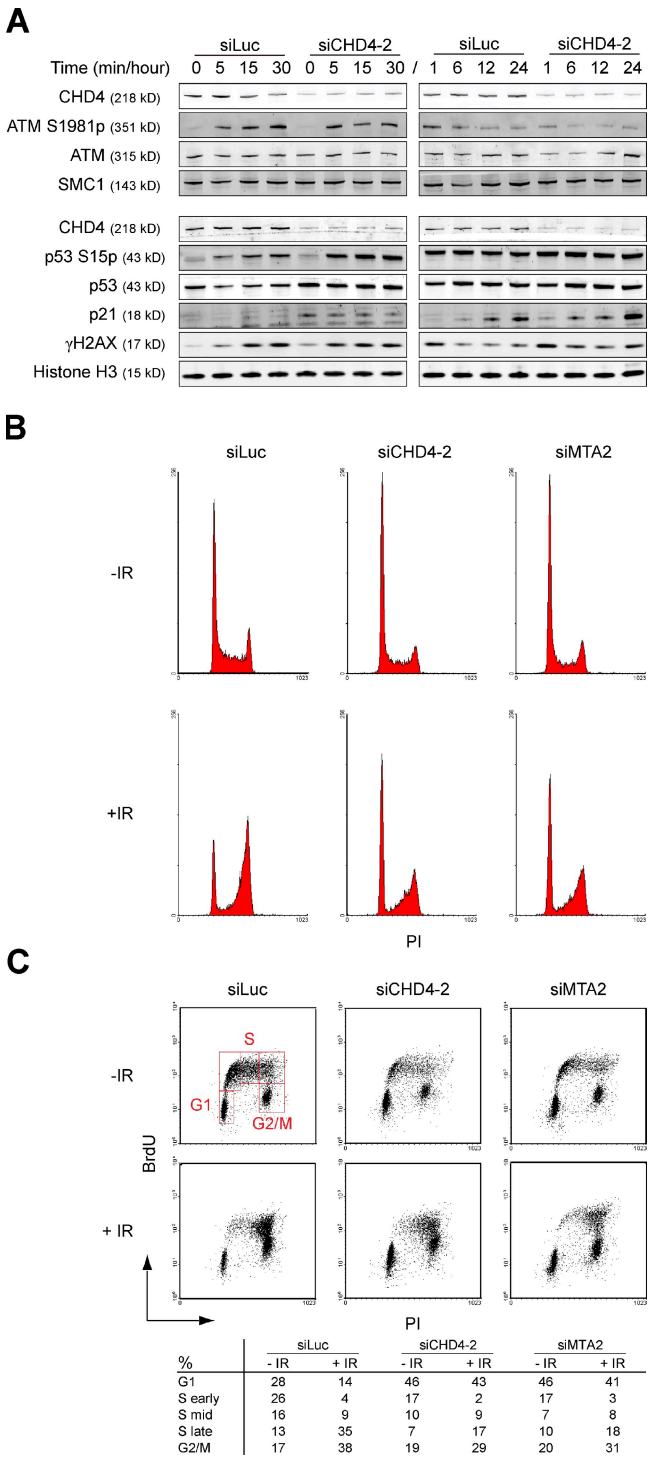

%	siLuc - IR	siLuc + IR	siCHD4-2 - IR	siCHD4-2 + IR	siMTA2 - IR	siMTA2 + IR
G1	28	14	46	43	46	41
S early	26	4	17	2	17	3
S mid	16	9	10	9	7	8
S late	13	35	7	17	10	18
G2/M	17	38	19	29	20	31

Figure 2. **CHD4 controls IR-induced p53/p21 responses.** (A) CHD4 depletion increases IR-induced p53 phosphorylation (S15p), p53, and p21 levels. U2OS cells were transfected with the indicated siRNAs and exposed to 6 Gy of IR. WCEs were prepared at the indicated time points and γH2AX, ATM S1981p, ATM, CHD4, p53 S15p, p53, and p21 levels were monitored by Western blot analysis. Histone H3 and SMC1 were loading controls. (B) CHD4- and MTA2-depleted cells accumulate in G1 phase and remain in G1 arrest after exposure to IR. U2OS cells were transfected with the indicated siRNAs for 72 h, exposed to 6 Gy of IR, and 12 h later, subjected to FACS. (C) As in B, except that cells were stained with BrdU. PI, propidium iodide.

NuRD rapidly accumulates within DSB-flanking chromatin

The DSB response is characterized by the accumulation of checkpoint and DNA repair proteins in DSB-flanking chromatin. To investigate whether NuRD plays a direct role in the DDR, we examined recruitment of several of its subunits (CHD4, MTA2, and MBD3) to sites of DNA damage. We found that GFP-tagged CHD4, MTA2, and MBD3 accumulate in microlaser-generated DSB tracks and span the entire chromatin region that was marked by γH2AX (Fig. 3 A and Fig. S2 A), a characteristic shared with other known DSB-associated factors (Bekker-Jensen et al., 2006). Furthermore, they were rapidly recruited to DSB tracks and accumulated with similar kinetics. Accumulation became detectable within 30 s, reaching half-maximum at 40 s and steady-state levels at 3 min (Fig. 3, B and C; and Fig. S2, B and C). Mailand et al. (2007) recently defined two distinct kinetic groups of proteins that arrive either early (e.g., MDC1 and RNF8) or late (e.g., BRCA1 and 53BP1) at the DSB track. We demonstrated that GFP-CHD4, MTA2-GFP, and GFP-MBD3 arrive at the DSB track as early as GFP-MDC1 (Fig. 3 C and Fig. S2 C). Interestingly, they reached their steady-state levels of accumulation significantly faster than MDC1 and BRCA1. This may suggest that these NuRD subunits do not occupy DSB-containing chromatin to the same level as these core components of the DSB response (Fig. 3 C and Fig. S2 C). We conclude that NuRD is among the factors that assemble early in DSB-flanking chromatin.

CHD4 regulates DSB-associated ubiquitylation to orchestrate the accumulation of RNF168 and BRCA1

To examine whether NuRD modulates early events of the DSB response, we analyzed IR-induced foci (IRIF) formation of γH2AX because this histone mark acts as a docking site for MDC1/RNF8 at DSBs (Stucki et al., 2005). However, CHD4 knockdown did not affect γH2AX IRIF formation (Fig. 4 A), which corroborates our Western blot analysis showing proper IR-induced γH2AX formation in the absence of CHD4 (Fig. 2 A and Fig. S1). Accordingly, MDC1 and RNF8 IRIF formation were also not affected by the loss of CHD4 (Fig. 4, A and B).

In contrast, the accumulation of conjugated ubiquitin into IRIF was impaired in CHD4-depleted cells (about twofold; Fig. 4, C and D). Consistently, we observed a distinct reduction in IRIF formation of RNF168 and BRCA1, which have been shown to bind to DSB-associated ubiquitin moieties (Fig. 4, C and D), the formation of which may require CHD4. Indeed, we found that CHD4 knockdown, like RNF8 knockdown, significantly decreased the level of γH2AX mono- and diubiquitylation after IR (Fig. S3, A and B; Huen et al., 2007). Because the total levels of endogenous MDC1, RNF8, RNF168, and BRCA1 were not affected by CHD4 depletion, we conclude that the observed defects in IRIF formation resulted from a reduction in RNF8/RNF168-dependent ubiquitylation and subsequent RNF168 and BRCA1 accumulation at DSBs (Fig. S1). Moreover, expression of a dominant-negative, ATPase-dead form of CHD4 (GFP-CHD4 K757R) reduced RNF168 IRIF formation (Fig. S3, C and D), suggesting that ATP-dependent chromatin remodeling driven by the CHD4 ATPase triggers this process.

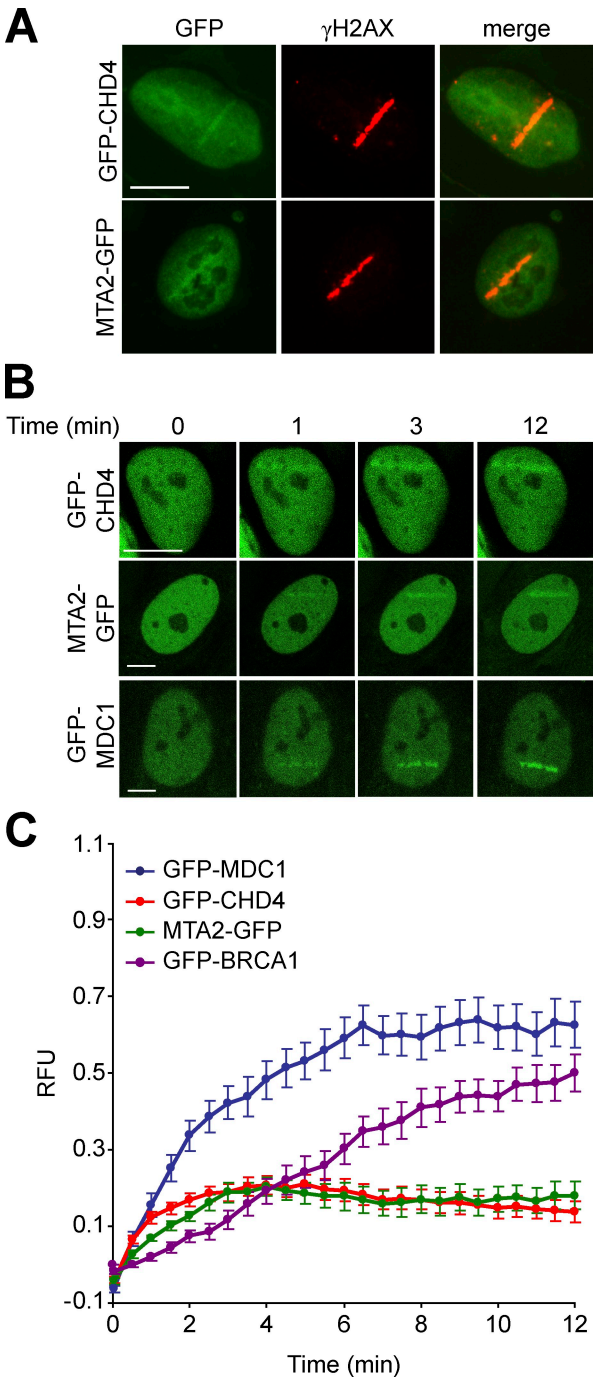

Figure 3. **CHD4 and MTA2 rapidly accumulate at sites of DNA damage.** (A) CHD4 and MTA2 accumulate in DSB-containing regions marked by γH2AX. U2OS cells transiently expressing GFP-CHD4 or MTA2-GFP were subjected to laser microirradiation. After 15 min, cells were immunostained for γH2AX. (B) GFP-CHD4 and MTA2-GFP, like GFP-MDC1, rapidly accumulate in DSB-containing regions. U2OS cells transiently expressing GFP-CHD4, MTA2-GFP, or GFP-MDC1 were microirradiated as in A and subjected to real-time recording of protein assembly at the damaged area. (C) Quantitative representation of the results in B. U2OS cells transiently expressing GFP-BRCA1 were included. Relative fluorescence units (RFU) are plotted on a time scale. Graphs represent the mean ± SEM of at least 10 individual cells from at least two independent experiments. Bars, 10 µm.

Thus, NuRD-mediated chromatin remodeling facilitates RNF8/RNF168-dependent histone ubiquitylation to orchestrate the accumulation of RNF168 and BRCA1. NuRD may change nucleosome structures such that the otherwise inaccessible RNF8/RNF168 H2A-type histone targets become amenable for ubiquitylation.

CHD4 and MTA2 promote DSB repair and G2/M checkpoint activation

RNF168 and BRCA1 promote DSB repair and G2/M checkpoint activation in response to IR (Moynahan et al., 1999; Xu et al., 2001; Xie et al., 2007; Doil et al., 2009; Stewart et al., 2009). Given that CHD4 facilitates the accumulation of these proteins in DSB-flanking chromatin, we examined its role in DSB repair and G2/M checkpoint activation.

Neutral comet assays were performed to determine the effect of CHD4 knockdown on the rejoining of IR-induced DSBs in VH10–telomerase reverse transcriptase (TERT) cells. As shown in Fig. 5 (A and B), we detected a pronounced increase in the level of DSBs in unirradiated CHD4-depleted cells. This is consistent with the aforementioned elevated levels of total γH2AX (Fig. 1 D and Fig. 2 A) and implies that spontaneous DSBs accumulate in the absence of CHD4 (Fig. 1 D). Importantly, the level of IR-induced DSBs remained higher at 2 h in CHD4 knockdown cells but returned to basal levels at 6 h. This suggests that CHD4 promotes proper DSB repair (Fig. 5, A and B).

Next, we tested the effect of CHD4 and MTA2 depletion on IR-induced G2/M checkpoint activation. We found that CHD4- and MTA2-depleted cells, like those depleted of BRCA1 or RNF8 (Xu et al., 2001; Huen et al., 2007; Kolas et al., 2007), failed to fully activate the G2/M checkpoint and continued to enter mitosis (Fig. 5, C and D), indicating that CHD4 and MTA2 facilitate full-scale activation of the G2/M checkpoint.

In conclusion, we report on the identification and characterization of the NuRD chromatin–remodeling complex as a novel factor involved in genome surveillance. The lack of CHD4 consistently led to increased levels of spontaneous DNA damage, a phenotype that was associated with the activation of p53 and p21 responses, reduced cell proliferation, and apoptosis. We propose that loss of chromatin remodeling by NuRD induces genome-wide chromatin alterations, which render chromatin more susceptible to spontaneous DNA breaks (Fig. 5 E). Support for such a scenario comes from a recent study, which demonstrated that loss of several NuRD components during premature and normal aging was associated with changes in higher-order chromatin structure, including loss of heterochromatic regions, and an accumulation of spontaneous DNA damage (Pegoraro et al., 2009).

We also provide evidence for a direct role of NuRD in the DSB response, as several NuRD components (CHD4, MTA2, and MBD3) assemble at DSBs. Loss of CHD4 uncoupled the DSB response at the level of RNF8/RNF168-mediated histone ubiquitylation, leading to defects in the assembly of RNF168 and BRCA1. This most likely attenuated DSB repair and activation of the G2/M checkpoint and contributed to the IR sensitivity observed in CHD4- or MTA2-depleted cells (Fig. 5 E). Thus, NuRD is a novel factor that preserves genome stability by modulating chromatin structure (a) genome-wide to prevent spontaneous DNA damage and (b) at DNA breaks to orchestrate a proper DSB response (see Larsen et al. in this issue). Our work

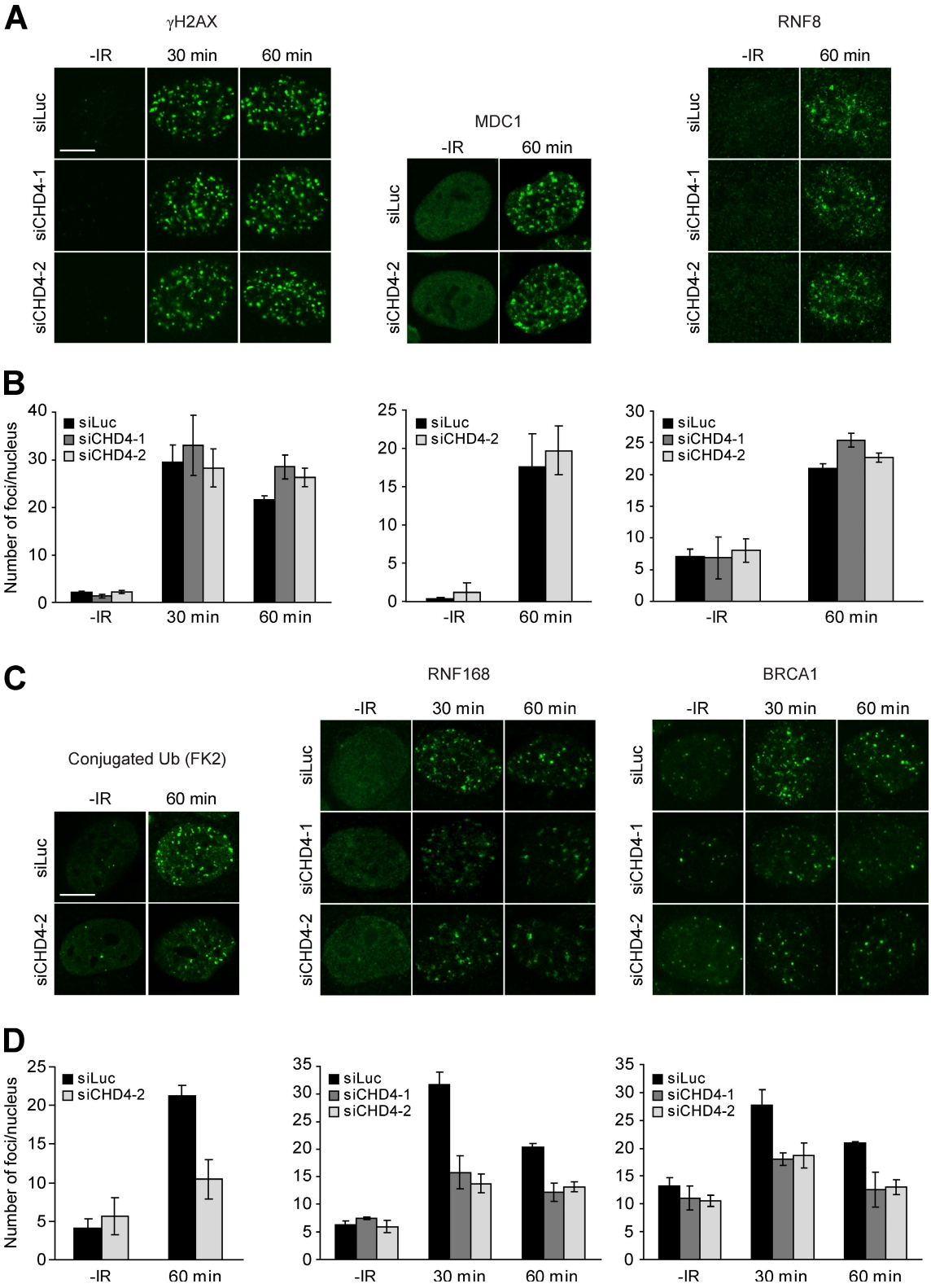

Figure 4. **CHD4 promotes histone ubiquitylation at DSBs to orchestrate the accumulation of RNF168 and BRCA1.** (A) CHD4 depletion does not alter γH2AX, MDC1, and RNF8 IRIF formation. Cells were transfected with the indicated siRNAs, exposed to 1 Gy of IR, and 30 and/or 60 min later, immunostained for γH2AX, MDC1, or RNF8. (B) Quantitative analysis of γH2AX, MDC1, and RNF8 IRIF formation. More than 150 nuclei from cells in A were scored per time point in at least two independent experiments. (C) CHD4 depletion impairs ubiquitin, RNF168, and BRCA1 IRIF formation. As in A, except that cells were immunostained for conjugated ubiquitin (FK2), RNF168, and BRCA1. (D) Quantitative analysis of ubiquitin, RNF168, and BRCA1 IRIF formation (as in B). Error bars indicate mean ± SEM. Bars, 10 µm.

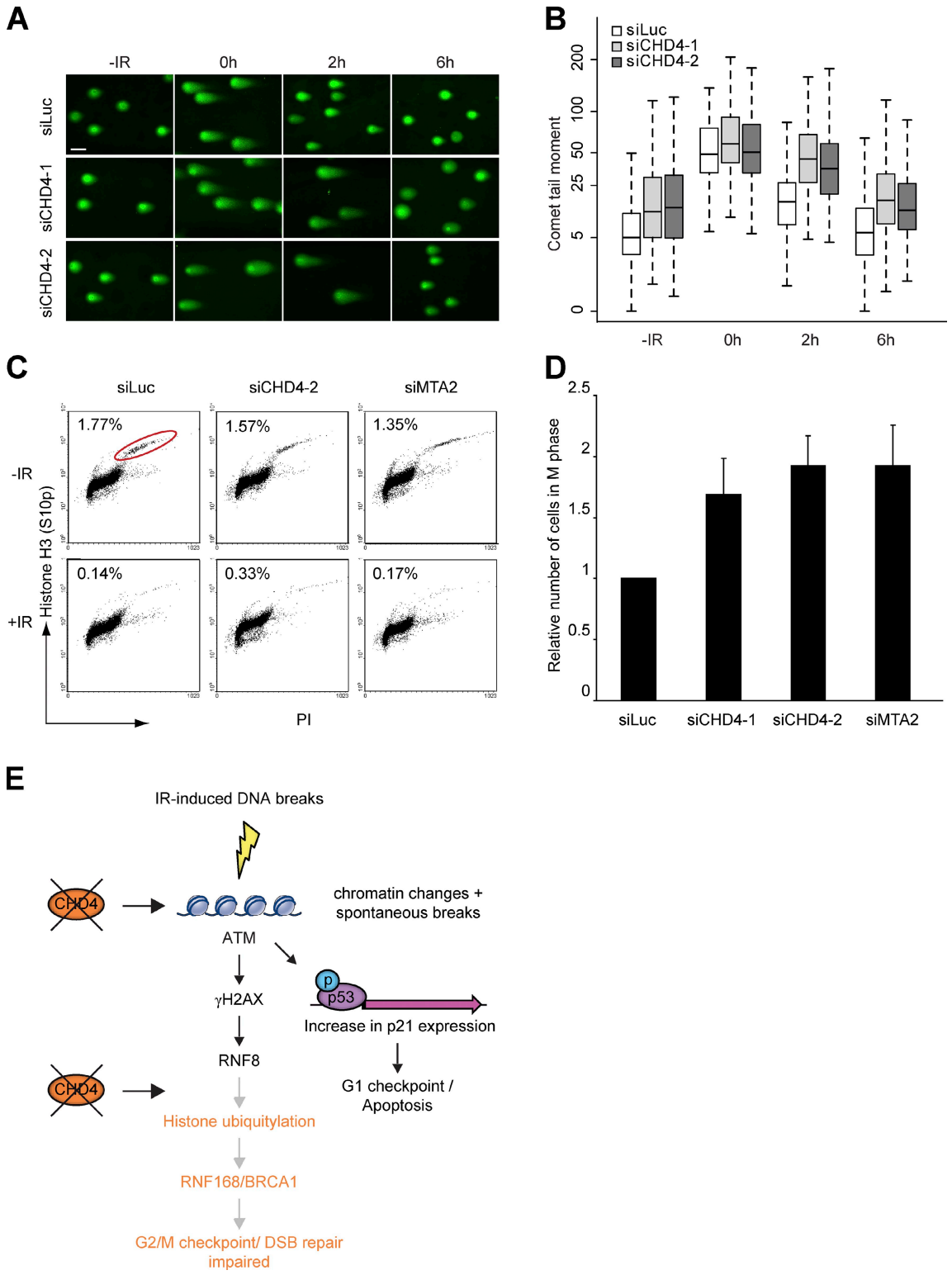

Figure 5. **CHD4 promotes DSB repair and IR-induced activation of the G2/M checkpoint.** (A) CHD4 depletion impairs DSB repair. VH10-TERT cells were transfected with the indicated siRNAs for 72 h, exposed to 20 Gy of IR, and subjected to neutral comet analysis at the indicated time points. Representative images are shown. Bar, 30 μm. (B) Quantification of tail moments using cells from A. Tail moments for each condition were calculated on a minimum of 300 cells for each data point. Results of four independent experiments are shown as a box and whisker plot. The ordinate is a cube root scale. Data were statistically analyzed using two-way analysis of variance, which revealed a significant delay in DSB repair for CHD4-depleted cells at 2 h after IR ($P < 0.0001$). (C) CHD4 or MTA2 depletion impairs IR-induced G2/M checkpoint activation. U2OS cells were transfected with the indicated siRNAs, exposed to 3 Gy of IR, and 1 h later, immunostained for phosphorylated histone H3 (S10p). Mitotic indexes were determined by FACS. A representative experiment is shown. PI, propidium iodide. Red circle indicates the fraction of M phase cells. (D) Graphical representation of relative mitotic index values. The ratio of index values from irradiated and unirradiated cells was calculated and normalized to that for control cells, which was set to 1. The mean ± SEM of four experiments is shown. (E) Model for the role of CHD4 in the maintenance of genome stability. See the last paragraph of Results and discussion for details.

provides a framework for future studies that will gain more insight in the cross talk between chromatin remodeling and mechanisms involved in genome maintenance.

Materials and methods

Cell culture and chemicals

Human U2OS, VH10-SV40–, and VH10-TERT–immortalized fibroblasts were grown in DME (Invitrogen) containing 10% FCS (Bodinco BV). siRNA and plasmid transfections were performed using HiPerfect (QIAGEN) and JetPEI (Polyplus Transfection), respectively, according to the manufacturer's instructions. The following siRNA sequences were used: (luciferase), 5′-CGUACGCGGAAUACUUCGA-3′; (CHD4-1; Thermo Fisher Scientific), 5′-CCAAGGACCUGAAUGAUGA-3′; (CHD4-2; Thermo Fisher Scientific), 5′-CAAAGGUGCUGCUGAUGUA-3′; (MTA2; Thermo Fisher Scientific), 5′-CAAAGUCUCUCUCCUUACAUU-3′; (RNF8; Thermo Fisher Scientific), 5′-GAGGGCCAAUGGACAAUUA-3′; and (XRCC4), 5′-AUAUGUUGGUGAACUGAGA-3′ (Sartori et al., 2007). Cells were examined 48 h after siRNA transfection unless otherwise stated. The cDNAs for human CHD4 (Thermo Fisher Scientific) and MTA2 (Imagenes) were cloned into pEGFP-C1 and pEGFP-N1, respectively (Takara Bio Inc.). The point mutation K757A was introduced into pEGFP-C1-CHD4 by site-directed mutagenesis. The pGFP-MBD3, GFP-BRCA1, and GFP-MDC1 constructs were provided by A. Bird (University of Edinburgh, Edinburgh, Scotland, UK), O. Sibon (University of Groningen, Groningen, Netherlands), and J. Lukas (Danish Cancer Society, Copenhagen, Denmark) respectively.

Generation of DSBs

DSBs were induced by IR, which was delivered by an x-ray generator (200 kV; 4 mA; 1.1 Gy/min dose rate; YXLON International).

Cell survival assay

VH10-SV40 cells were transfected for 48 h, trypsinized, seeded at low density, and exposed to IR. 7 d later, cells were washed with 0.9% NaCl and stained with methylene blue. Colonies of >20 cells were scored.

Microscopy and laser microirradiation

Brightfield pictures were taken with a fluorescence microscope (EVOS fl AMG; Westover Scientific) using the 4× Ph objective. Laser microirradiation was performed on a confocal microscope (TCS SP5/AOBS; Leica) equipped with an environmental chamber set to 37°C and 5% CO_2. Cells were grown on glass-bottom dishes (MatTek) in colorless medium containing 10% FCS (Invitrogen), and Hoechst 33342 was added to the medium at a concentration of 0.5 µg/ml before laser irradiation. 0.5 × 10 µm DSB-containing tracks were generated with a diode laser (λ = 405 nm; 30% laser power; 0.75-s irradiation time; 2,220 µW) using a UV-transmitting 63× 1.4 NA oil immersion objective (HCX PL APO; Leica). Confocal images were recorded before and after laser irradiation at 20- or 30-s time intervals over a period of 5 or 12 min and analyzed using LAS-AF software (Leica). Fluorescence intensities were corrected for background and normalized to prebleach values to determine recruitment kinetics.

Antibodies

IRIF and Western blot analysis were performed using antibodies to γH2AX (Millipore), α-tubulin (Sigma-Aldrich), ATM (GeneTex), ubiquitin (FK2; Enzo Life Sciences, Inc.), BRCA1 (EMD), histone H3, ATM S1981p, MDC1, MTA2, CHD4, and RNF8 (Abcam), p53 and p21 (Santa Cruz Biotechnology, Inc.), p53 S15p (Cell Signaling Technology), and SMC1 (Bethyl Laboratories). The antibodies to RNF168 and XRCC4 were provided by D. Durocher (University of Toronto, Toronto, Ontario, Canada) and M. Modesti (Universite d'Aix-Marseille, Marseille, France), respectively.

IRIF analysis

Cells were grown on glass coverslips and treated as indicated in Figs. 1–5. Subsequently, cells were washed with PBS, fixed with 2% formaldehyde and 0.25% Triton X-100 in PBS, and incubated with appropriate primary and secondary antibodies (Alexa Fluor 488 [Invitrogen] or goat anti–rabbit IgG conjugated to Cy3 [Jackson ImmunoResearch Laboratories, Inc.]) and DAPI. An additional extraction with 0.25% Triton X-100 in CSK buffer (10 mM Hepes, 300 mM sucrose, 100 mM NaCl, and 3 mM $MgCl_2$) was performed before fixation and incubation with primary antibodies against RNF168 and BRCA1. Images were recorded with a microscope (Axioplan; Carl Zeiss, Inc.) using a 63× 1.25 NA oil objective and a camera (AxioCam mRm; Carl Zeiss, Inc.) and analyzed using home-made Stacks software. Nuclei were detected and selected by global thresholding of DAPI images. Contour tracing was performed, after which pixels were labeled with a unique object index that determines to which nucleus the pixels belong. The actual detection of foci was performed on Alexa Fluor 488 or Cy3 images. First, a top-hat transformation was performed to reduce the influence of variation in background staining within nuclei. On the resulting image, a watershed algorithm was performed to determine the location of foci within the image by providing a unique spot index to the pixels of each focus. By combining foci indices with object indices obtained from the DAPI image, foci could be assigned to the nuclei in which they were detected, allowing calculation of the number of foci per nucleus.

Chromatin fractionation and Western blotting

Chromatin-enriched extracts were prepared and used for immunoprecipitation as described previously (Huen et al., 2007). Whole cell extracts (WCEs) were prepared by cell lysis in Laemmli buffer. Proteins were separated in Bis-Tris-HCl–buffered acrylamide gels (Invitrogen) and blotted onto either PVDF (Millipore) or nitrocellulose (GE Healthcare). Membranes were incubated with primary antibody as indicated in Figs. 1–5 followed by incubation with secondary antibody (Odyssey IRDye; LI-COR Biosciences). The Odyssey imager (LI-COR Biosciences) equipped with Odyssey software (version 3.0) was used to scan the membranes and analyze the fluorescence signals.

FACS

For G2/M checkpoint analysis, cells were fixed in 70% ethanol and stained with rabbit antibody to histone H3 S10p (Millipore) followed by incubation with conjugated anti–rabbit IgG (Alexa Fluor 488). For cell cycle analysis, cells were pulse labeled with 10 µM BrdU for 1 h, fixed in 70% ethanol, denatured in 2 M HCl, and stained with mouse antibody to BrdU followed by incubation with conjugated anti–mouse IgG (Alexa Fluor 488) and DNA staining with 0.1 mg/ml propidium iodide. Cell sorting was performed on a flow cytometer (LSRII; BD) using FACSDiva software (version 5.0.3; BD). Quantifications were performed using WinMDI software (version 2.9; J. Trotter).

Neutral comet assay

DSBs were measured in VH10-TERT cells using the Comet Assay system (Trevigen) according to the manufacturer's instructions. Comet tail moments were scored using Comet Score software (TriTek).

Online supplemental material

Fig. S1 shows that depletion of CHD4 does not alter the expression level of DDR proteins after IR. Fig. S2 shows that MBD3-GFP rapidly accumulates at sites of laser-induced DNA damage. Fig. S3 shows that CHD4 depletion reduces IR-induced γH2AX ubiquitylation and that CHD4 ATPase activity is required for RNF168 IRIF formation. Online supplemental material is available at http://www.jcb.org/cgi/content/full/jcb.201001048/DC1.

We thank Jiri Lukas, Dan Durocher, Adrian Bird, Ody Sibon, and Mauro Modesti for providing reagents. We acknowledge Ron Romeijn for constructing pEGFP-C1-MTA2, Antoine de Morrée for technical advice, Karien Wiesmeijer, Annelies van der Laan, Roeland Dirks, Przemek Krawczyk, and Jacob Aten for assistance with the microlaser irradiation, and Jiri Lukas for sharing results before publication.

This work was supported by a Vidi grant from the Netherlands Organization for Scientific Research (NWO).

Submitted: 11 January 2010
Accepted: 6 August 2010

References

Ahel, D., Z. Horejsí, N. Wiechens, S.E. Polo, E. Garcia-Wilson, I. Ahel, H. Flynn, M. Skehel, S.C. West, S.P. Jackson, et al. 2009. Poly(ADP-ribose)-dependent regulation of DNA repair by the chromatin remodeling enzyme ALC1. *Science.* 325:1240–1243. doi:10.1126/science.1177321

Bekker-Jensen, S., C. Lukas, R. Kitagawa, F. Melander, M.B. Kastan, J. Bartek, and J. Lukas. 2006. Spatial organization of the mammalian genome surveillance machinery in response to DNA strand breaks. *J. Cell Biol.* 173:195–206. doi:10.1083/jcb.200510130

Chai, B., J. Huang, B.R. Cairns, and B.C. Laurent. 2005. Distinct roles for the RSC and Swi/Snf ATP-dependent chromatin remodelers in DNA double-strand break repair. *Genes Dev.* 19:1656–1661. doi:10.1101/gad.1273105

Clapier, C.R., and B.R. Cairns. 2009. The biology of chromatin remodeling complexes. *Annu. Rev. Biochem.* 78:273–304. doi:10.1146/annurev.biochem.77.062706.153223

Denslow, S.A., and P.A. Wade. 2007. The human Mi-2/NuRD complex and gene regulation. *Oncogene.* 26:5433–5438. doi:10.1038/sj.onc.1210611

Doil, C., N. Mailand, S. Bekker-Jensen, P. Menard, D.H. Larsen, R. Pepperkok, J. Ellenberg, S. Panier, D. Durocher, J. Bartek, et al. 2009. RNF168 binds and amplifies ubiquitin conjugates on damaged chromosomes to allow accumulation of repair proteins. *Cell.* 136:435–446. doi:10.1016/j.cell.2008.12.041

Dubrana, K., H. van Attikum, F. Hediger, and S.M. Gasser. 2007. The processing of double-strand breaks and binding of single-strand-binding proteins RPA and Rad51 modulate the formation of ATR-kinase foci in yeast. *J. Cell Sci.* 120:4209–4220. doi:10.1242/jcs.018366

Gong, Z., Y.W. Cho, J.E. Kim, K. Ge, and J. Chen. 2009. Accumulation of Pax2 transactivation domain interaction protein (PTIP) at sites of DNA breaks via RNF8-dependent pathway is required for cell survival after DNA damage. *J. Biol. Chem.* 11:7284–7293. doi:10.1074/jbc.M809158200

Gottschalk, A.J., G. Timinszky, S.E. Kong, J. Jin, Y. Cai, S.K. Swanson, M.P. Washburn, L. Florens, A.G. Ladurner, J.W. Conaway, and R.C. Conaway. 2009. Poly(ADP-ribosyl)ation directs recruitment and activation of an ATP-dependent chromatin remodeler. *Proc. Natl. Acad. Sci. USA.* 106:13770–13774. doi:10.1073/pnas.0906920106

Grawunder, U., D. Zimmer, S. Fugmann, K. Schwarz, and M.R. Lieber. 1998. DNA ligase IV is essential for V(D)J recombination and DNA double-strand break repair in human precursor lymphocytes. *Mol. Cell.* 2:477–484. doi:10.1016/S1097-2765(00)80147-1

Hoeijmakers, J.H. 2001. Genome maintenance mechanisms for preventing cancer. *Nature.* 411:366–374. doi:10.1038/35077232

Huang, J., M.S. Huen, H. Kim, C.C. Leung, J.N. Glover, X. Yu, and J. Chen. 2009. RAD18 transmits DNA damage signalling to elicit homologous recombination repair. *Nat. Cell Biol.* 11:592–603. doi:10.1038/ncb1865

Huen, M.S., R. Grant, I. Manke, K. Minn, X. Yu, M.B. Yaffe, and J. Chen. 2007. RNF8 transduces the DNA-damage signal via histone ubiquitylation and checkpoint protein assembly. *Cell.* 131:901–914. doi:10.1016/j.cell.2007.09.041

Ikura, T., S. Tashiro, A. Kakino, H. Shima, N. Jacob, R. Amunugama, K. Yoder, S. Izumi, I. Kuraoka, K. Tanaka, et al. 2007. DNA damage-dependent acetylation and ubiquitination of H2AX enhances chromatin dynamics. *Mol. Cell. Biol.* 27:7028–7040. doi:10.1128/MCB.00579-07

Jazayeri, A., J. Falck, C. Lukas, J. Bartek, G.C. Smith, J. Lukas, and S.P. Jackson. 2006. ATM- and cell cycle-dependent regulation of ATR in response to DNA double-strand breaks. *Nat. Cell Biol.* 8:37–45. doi:10.1038/ncb1337

Khanna, K.K., and S.P. Jackson. 2001. DNA double-strand breaks: signaling, repair and the cancer connection. *Nat. Genet.* 27:247–254. doi:10.1038/85798

Kolas, N.K., J.R. Chapman, S. Nakada, J. Ylanko, R. Chahwan, F.D. Sweeney, S. Panier, M. Mendez, J. Wildenhain, T.M. Thomson, et al. 2007. Orchestration of the DNA-damage response by the RNF8 ubiquitin ligase. *Science.* 318:1637–1640. doi:10.1126/science.1150034

Larsen, D.H., C. Poinsignon, T. Gudjonsson, C. Dinant, M.R. Payne, F.J. Hari, J.M.R. Danielsen, P. Menard, J.C. Sand, M. Stucki, et al. 2010. The chromatin-remodeling factor CHD4 coordinates signaling and repair after DNA damage. *J. Cell Biol.* 190:731–740.

Liang, B., J. Qiu, K. Ratnakumar, and B.C. Laurent. 2007. RSC functions as an early double-strand-break sensor in the cell's response to DNA damage. *Curr. Biol.* 17:1432–1437. doi:10.1016/j.cub.2007.07.035

Luo, J., F. Su, D. Chen, A. Shiloh, and W. Gu. 2000. Deacetylation of p53 modulates its effect on cell growth and apoptosis. *Nature.* 408:377–381. doi:10.1038/35042612

Mailand, N., S. Bekker-Jensen, H. Faustrup, F. Melander, J. Bartek, C. Lukas, and J. Lukas. 2007. RNF8 ubiquitylates histones at DNA double-strand breaks and promotes assembly of repair proteins. *Cell.* 131:887–900. doi:10.1016/j.cell.2007.09.040

Morrison, A.J., J. Highland, N.J. Krogan, A. Arbel-Eden, J.F. Greenblatt, J.E. Haber, and X. Shen. 2004. INO80 and gamma-H2AX interaction links ATP-dependent chromatin remodeling to DNA damage repair. *Cell.* 119:767–775. doi:10.1016/j.cell.2004.11.037

Moynahan, M.E., J.W. Chiu, B.H. Koller, and M. Jasin. 1999. Brca1 controls homology-directed DNA repair. *Mol. Cell.* 4:511–518. doi:10.1016/S1097-2765(00)80202-6

Murr, R., J.I. Loizou, Y.G. Yang, C. Cuenin, H. Li, Z.Q. Wang, and Z. Herceg. 2006. Histone acetylation by Trrap-Tip60 modulates loading of repair proteins and repair of DNA double-strand breaks. *Nat. Cell Biol.* 8:91–99. doi:10.1038/ncb1343

Papamichos-Chronakis, M., J.E. Krebs, and C.L. Peterson. 2006. Interplay between Ino80 and Swr1 chromatin remodeling enzymes regulates cell cycle checkpoint adaptation in response to DNA damage. *Genes Dev.* 20:2437–2449. doi:10.1101/gad.1440206

Park, J.H., E.J. Park, H.S. Lee, S.J. Kim, S.K. Hur, A.N. Imbalzano, and J. Kwon. 2006. Mammalian SWI/SNF complexes facilitate DNA double-strand break repair by promoting gamma-H2AX induction. *EMBO J.* 25:3986–3997. doi:10.1038/sj.emboj.7601291

Pegoraro, G., N. Kubben, U. Wickert, H. Göhler, K. Hoffmann, and T. Misteli. 2009. Ageing-related chromatin defects through loss of the NURD complex. *Nat. Cell Biol.* 11:1261–1267. doi:10.1038/ncb1971

Sartori, A.A., C. Lukas, J. Coates, M. Mistrik, S. Fu, J. Bartek, R. Baer, J. Lukas, and S.P. Jackson. 2007. Human CtIP promotes DNA end resection. *Nature.* 450:509–514. doi:10.1038/nature06337

Seelig, H.P., I. Moosbrugger, H. Ehrfeld, T. Fink, M. Renz, and E. Genth. 1995. The major dermatomyositis-specific Mi-2 autoantigen is a presumed helicase involved in transcriptional activation. *Arthritis Rheum.* 38:1389–1399. doi:10.1002/art.1780381006

Shiloh, Y. 2003. ATM and related protein kinases: safeguarding genome integrity. *Nat. Rev. Cancer.* 3:155–168. doi:10.1038/nrc1011

Shim, E.Y., J.L. Ma, J.H. Oum, Y. Yanez, and S.E. Lee. 2005. The yeast chromatin remodeler RSC complex facilitates end joining repair of DNA double-strand breaks. *Mol. Cell. Biol.* 25:3934–3944. doi:10.1128/MCB.25.10.3934-3944.2005

Shim, E.Y., S.J. Hong, J.H. Oum, Y. Yanez, Y. Zhang, and S.E. Lee. 2007. RSC mobilizes nucleosomes to improve accessibility of repair machinery to the damaged chromatin. *Mol. Cell. Biol.* 27:1602–1613. doi:10.1128/MCB.01956-06

Stewart, G.S., S. Panier, K. Townsend, A.K. Al-Hakim, N.K. Kolas, E.S. Miller, S. Nakada, J. Ylanko, S. Olivarius, M. Mendez, et al. 2009. The RIDDLE syndrome protein mediates a ubiquitin-dependent signaling cascade at sites of DNA damage. *Cell.* 136:420–434. doi:10.1016/j.cell.2008.12.042

Stucki, M., J.A. Clapperton, D. Mohammad, M.B. Yaffe, S.J. Smerdon, and S.P. Jackson. 2005. MDC1 directly binds phosphorylated histone H2AX to regulate cellular responses to DNA double-strand breaks. *Cell.* 123:1213–1226. doi:10.1016/j.cell.2005.09.038

Tsukuda, T., A.B. Fleming, J.A. Nickoloff, and M.A. Osley. 2005. Chromatin remodelling at a DNA double-strand break site in *Saccharomyces cerevisiae. Nature.* 438:379–383. doi:10.1038/nature04148

van Attikum, H., and S.M. Gasser. 2009. Crosstalk between histone modifications during the DNA damage response. *Trends Cell Biol.* 19:207–217. doi:10.1016/j.tcb.2009.03.001

van Attikum, H., O. Fritsch, B. Hohn, and S.M. Gasser. 2004. Recruitment of the INO80 complex by H2A phosphorylation links ATP-dependent chromatin remodeling with DNA double-strand break repair. *Cell.* 119:777–788. doi:10.1016/j.cell.2004.11.033

van Attikum, H., O. Fritsch, and S.M. Gasser. 2007. Distinct roles for SWR1 and INO80 chromatin remodeling complexes at chromosomal double-strand breaks. *EMBO J.* 26:4113–4125. doi:10.1038/sj.emboj.7601835

van Haaften, G., R. Romeijn, J. Pothof, W. Koole, L.H. Mullenders, A. Pastink, R.H. Plasterk, and M. Tijsterman. 2006. Identification of conserved pathways of DNA-damage response and radiation protection by genome-wide RNAi. *Curr. Biol.* 16:1344–1350. doi:10.1016/j.cub.2006.05.047

Wang, B., and S.J. Elledge. 2007. Ubc13/Rnf8 ubiquitin ligases control foci formation of the Rap80/Abraxas/Brca1/Brcc36 complex in response to DNA damage. *Proc. Natl. Acad. Sci. USA.* 104:20759–20763. doi:10.1073/pnas.0710061104

Wang, H.B., and Y. Zhang. 2001. Mi2, an auto-antigen for dermatomyositis, is an ATP-dependent nucleosome remodeling factor. *Nucleic Acids Res.* 29:2517–2521. doi:10.1093/nar/29.12.2517

Xie, A., A. Hartlerode, M. Stucki, S. Odate, N. Puget, A. Kwok, G. Nagaraju, C. Yan, F.W. Alt, J. Chen, et al. 2007. Distinct roles of chromatin-associated proteins MDC1 and 53BP1 in mammalian double-strand break repair. *Mol. Cell.* 28:1045–1057. doi:10.1016/j.molcel.2007.12.005

Xu, B., Kim St, and M.B. Kastan. 2001. Involvement of Brca1 in S-phase and G(2)-phase checkpoints after ionizing irradiation. *Mol. Cell. Biol.* 21:3445–3450. doi:10.1128/MCB.21.10.3445-3450.2001

Xue, Y., J. Wong, G.T. Moreno, M.K. Young, J. Côté, and W. Wang. 1998. NURD, a novel complex with both ATP-dependent chromatin-remodeling and histone deacetylase activities. *Mol. Cell.* 2:851–861. doi:10.1016/S1097-2765(00)80299-3

Zhang, Y., H.H. Ng, H. Erdjument-Bromage, P. Tempst, A. Bird, and D. Reinberg. 1999. Analysis of the NuRD subunits reveals a histone deacetylase core complex and a connection with DNA methylation. *Genes Dev.* 13:1924–1935. doi:10.1101/gad.13.15.1924

Zou, L., and S.J. Elledge. 2003. Sensing DNA damage through ATRIP recognition of RPA-ssDNA complexes. *Science.* 300:1542–1548. doi:10.1126/science.1083430